FIG. 5. (a) Block diagram of a complete mold-to-wafer alignment system for imprint lithography showing all of the major components (alignment microscopes, photodetectors, computer, digital drive electronics, and adaptive mold holder). (b) A block diagram of the system used to harden the polymer with UV radiation after the alignment optics have been removed.

reproduce the x and y offsets shown in Fig. 3(b). However, even with a frictional coefficient of 1.0, the forces on some segments were close to the maximum vacuum hold-down force (14.696 lb/in.^{2}×0.5 in.^{2}). Therefore, we have concluded that larger wafer distortions can be accommodated with an adaptive mold holder rather than with an adaptive wafer holder.

IV. ALIGNMENT SYSTEM

A block diagram of a complete mold-to-wafer alignment system for imprint lithography is shown in Fig. 5(a). The space between a rigid fused-silica mold and a silicon wafer is filled with a low viscosity (~1 cP) photopolymer precursor and pressure is applied until the mold almost touches the wafer. An array of alignment microscopes image pairs of alignment marks (one on the mold and one on the wafer) at three or more sites within an exposure field onto an array of split photodetectors (described in Sec. II). Error signals produced by those detectors are fed to a computer that controls the voltages on an adaptive mold holder (described in Sec. III). While the photopolymer is still a low viscosity liquid, the piezoelectric actuators in the adaptive mold holder deliberately distort the mold so that all of the alignment-mark

pairs are brought into registration (within the required tolerance) simultaneously. The piezoelectric actuators will have time constants of the order of milliseconds. If the integration time in the photodetectors is tens of milliseconds, the alignment system should settle in less than a tenth of a second. Once alignment is achieved over the entire exposure field, mold and wafer are locked together while the voltages on the piezoelectric actuators are held constant and the alignment optics are removed. The photopolymer is exposed to UV radiation through the back of the transparent mold, as shown in Fig. 5(b), and is hardened. Alternatively, it may be possible to introduce the UV radiation needed to cure the photopolymer via a dichroic beam splitter, in which case, the alignment system could remain active even during the flood exposure. This would eliminate errors due to heating effects during UV exposure or drift in the piezoelectrics.

It has been tacitly assumed in all of this that misalignment is a continuously varying quantity and is not characterized by sudden jumps. In other words, if the alignment marks are close enough together and they are in alignment after the mold has been deformed, then the area between them will also be in good alignment. This is important because, to produce a product with nonzero yield, pattern overlay must be within the alignment tolerance at all points in the image field, not just at the alignment marks.

ACKNOWLEDGMENT

[1]S. Y. Chou, P. R. Krauss, W. Zhang, L. Guo, and L. Zhuang, J. Vac. Sci. Technol. B 15, 2897 (1997).
[2]M. Colburn et al., Proc. SPIE 3676, 379 (1999).
[3]M. Colburn, A. Grot, M. Amistoso, B. J. Choi, T. Bailey, J. Ekerdt, S. V. Sreenivasan, J. Hollenhorst and C. G. Willson, Paper 3997-49 at SPIE's 25th Annual International Symposium on Microlithography, 27 Feb.–3 March 2000, Santa Clara, CA.
[4]Y. Xia, J. J. McClelland, R. Gupta, D. Qin, X.-M. Zhao, L. L. Sohn, R. J. Celotta, and G. M. Whitesides, Adv. Mater. 9, 147 (1997).
[5]D. C. Flanders, H. I. Smith, and S. Austin, Appl. Phys. Lett. 31, 426 (1977).
[6]Y. Torii and Y. Mizushima, Opt. Commun. 23, 135 (1977).
[7]S. Austin, H. I. Smith, and D. C. Flanders, J. Vac. Sci. Technol. 15, 984 (1978).
[8]D. L. White, M. Feldman, T. E. Saunders, and P. Gunter, J. Vac. Sci. Technol. B 6, 1921 (1988).
[9]S. Stanton, D. L. White, and G. Zipfel, J. Vac. Sci. Technol. B 6, 2665 (1995).
[10]A. Wong, Rigorous Three-Dimensional Time-Domain Finite-Difference Electromagnetic Simulation (Electronics Research Laboratory, University of California, Berkeley, CA, 1994).
[11]Bio-Rad Semiconductor Measurements Division, 520 Clyde Avenue, Mountain View, CA 94043.
[12]Algor, Inc., 150 Beta Drive, Pittsburgh, PA 15238.

Mean X UL: -0.012 μm
Mean Y UL: -0.042 μm
Mean X UR: +0.030 μm
Mean Y UR: -0.059 μm
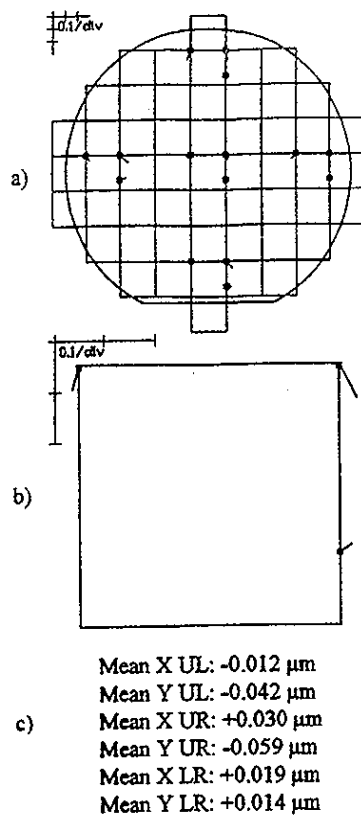Mean X LR: +0.019 μm
Mean Y LR: +0.014 μm

FIG. 3. x and y offsets (a) in five exposure fields on a typical device wafer recorded with a Bio-Rad Model Q200 overlay metrology tool displayed as a vector map and in one field representing an average of the five measured fields; (b) displayed as a vector map, and (c) as numerical values for the upper left (UL), upper right (UR), and lower right (LR) alignment mark locations.

FIG. 4. (a) Sketch of an adaptive mold holder for a 1.25 in.×1.25 in.×0.090 in. thick fused-silica imprint mold showing the location of its eight piezoelectric actuators and the forces required to produce x and y surface displacements that exactly reproduce the x and y offset data provided in Fig. 3(c) and (b) a plot of the in-plane surface displacements for this mold with the same loads computed using a commercially available finite-element linear-stress-analysis code (displacement values are in inches).

electric actuators in an adaptive mold holder like the one shown in Fig. 4(a). The deformations required to cancel the measured misalignments at three sites can be computed analytically by solving six simultaneous equations involving six known displacements, e.g., the x and y misalignments at the three alignment mark sites shown in Fig. 3(b), and the six unknown orthogonal strains (magnification, shear, and trapezoidal distortion in the x and y directions). Knowing the strains required for alignment, we can then apply the proper voltages to the piezoelectric actuators to create those strains and bring the mold and wafer into alignment simultaneously at all three alignment marks.

We have checked our analytical solution to the problem of determining the required strains using a finite-element linear-stress-analysis code from Algor[12] to simulate the behavior of a 1.25 in.×1.25 in.×0.090 in. thick fused-silica mold (elastic modulus=1.04×10^7 lb/in.^{2}, Poisson's ratio =0.17) loaded on its edges with the forces shown in Fig. 4(a). A plot of the in-plane surface displacements from a simulation that exactly reproduced the measured x and y offsets at the three sites shown in Fig. 3(b) is shown in Fig.
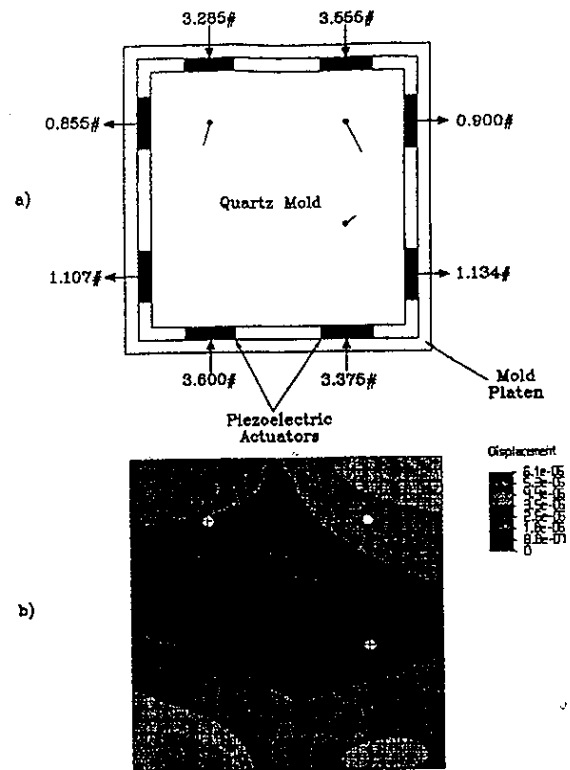
4(b). Not surprisingly, the results from the analytical solution to the six simultaneous equations and those from the finite-element analysis (FEA) simulation were quite similar. The only differences were in areas of the mold near the actuators (lying outside of the patterned area) and were a result of the overly simplistic boundary conditions assumed in the analytical model. For completeness, we also used the finite-element code to simulate the behavior of a silicon wafer (elastic modulus=2.36×10^7 lb/in.^{2}, Poisson's ratio=0.22) on an adaptive wafer holder. The adaptive wafer holder was assumed to be divided into a number of square segments, each with a cross sectional area of 0.5 in.^{2} and with a vacuum port to hold the wafer. Two piezoelectric actuators per side allowed each segment to be distorted in a variety of ways, from simple x and y displacements to complex changes in shape (magnification, shear, rotation, etc.). It was found from the FEA model of the silicon wafer on the adaptive wafer holder that the most uniform distribution of surface displacements on the silicon wafer was created by applying forces to all segments except those directly under the exposure site. With this arrangement we were again able to
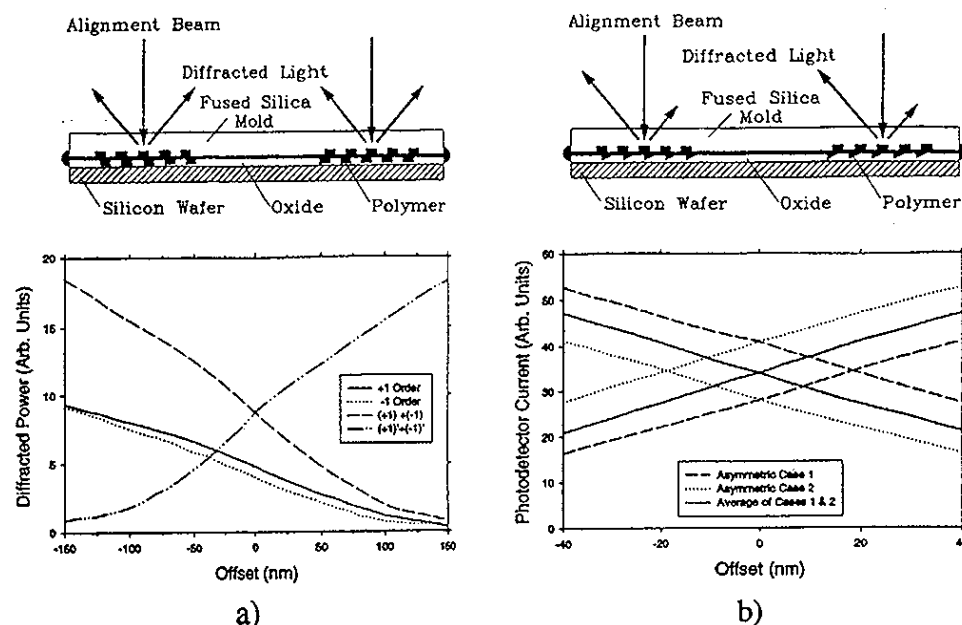
FIG. 2. Sketches of alignment-metrology techniques for use with imprint lithography when the grating alignment marks are in similar materials, i.e., in fused silica and in an oxide layer, and the gratings are (a) highly symmetric and (b) highly asymmetric together with results derived from a ray trace at 365 nm wavelength of a double pass through identical mold and wafer grating alignment marks (period=0.6 μm, depth=50 nm and refractive index=1.5) separated by a 20 nm wide gap filled with a polymer with refractive index=1.9. In (a) alignment is determined by balancing the total power diffracted into the first orders of the two different grating pairs (dashed and dash-dotted curves). In (b) the wafer grating lines produce an erroneous offset because they are asymmetrical (dotted curves). A second set of alignment marks opposite in phase from the first produce an equal but opposite offset (dashed curves). The average of the two is the correct alignment (solid curves).

two orthogonal in-plane directions and four split photodetectors. Since split photodiodes can produce identical amplification to better than 1%, the alignment sensitivity for such a technique should be in the nanometer range. The only errors, beside those due to the alignment-system optics (which we believe can be made quite small), will be those due to the relative distortion between the mold and the wafer patterns.

III. DISTORTION CORRECTION

The mold and the wafer will tend to have distortions due to imperfect fabrication and to internal strains from prior processing steps. Thus, an alignment mark at one site on a mold might be brought to within 10 nm of the corresponding mark on the wafer, but, due to wafer distortion, an alignment mark at another site could still be several hundred nanometers out of alignment. Any attempt to bring a second pair of marks into alignment would destroy the registration at the first site. Although alignment metrology in imprint lithography is inherently superior to that used in conventional projection lithography, neither can do much about pattern distortion. In conventional projection lithography, a small improvement in yield can be made by exposing the lead wafer in a lot and measuring the resulting overlay errors between the mask and wafer patterns offline (at, typically, three sites per exposure field and five exposure fields per wafer) with an overlay metrology tool such as the Bio-Rad Model Q200.[11] A vector map of the x and y offsets of a

"typical" device wafer recorded with such a tool is shown in Fig. 3(a). The map shows that there are long-range distortions over several exposure fields (notice the left/right asymmetry evident in the center row of exposures). These can be caused by stresses in the patterning layers, thermal gradients over the wafer during processing, systematic errors in the $x-y$ stages, differences in speed between mask and wafer in a scanner, etc. The vector map of the average x and y offsets for all fields reproduced in Fig. 3(b) shows that data from each site within a single exposure field can be quite different and that a single $x-y$ wafer displacement can not bring all three sites into alignment simultaneously. In practice, overlay-error data like those shown in Fig. 3(c) are used to determine an average set of corrections to apply to a projection stepper. These corrections, typically, x translation, y translation, field magnification, and field rotation, are set just once at the beginning of a run of wafers and are applied equally at all exposure fields. One would like to use different corrections for each field, but such a process is considered to be too time consuming and, as is evident from the data shown in Fig. 3, would still not result in perfect alignment.

Instead of trying to make distortion-free molds and wafers, very likely an impossible task, a more reasonable solution is to deliberately deform the mold (or the wafer) to make the mold and wafer patterns more congruent. For example, an imprint mold can be deformed in a highly controlled way by applying precisely the right voltage to each of the
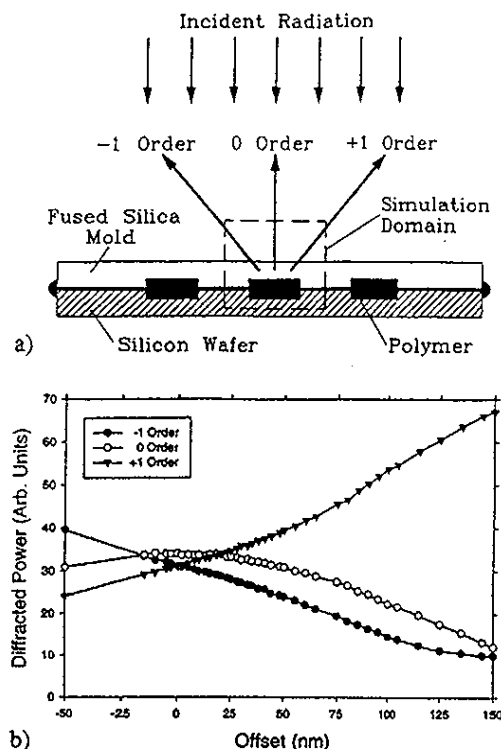
Incident Radiation

a)

b)

FIG. 1. (a) Sketch of an alignment-metrology technique for use with imprint lithography when the grating alignment marks (period=0.6 μm, depth=50 nm) are in dissimilar materials, i.e., fused silica and silicon, forming a strongly blazed grating and (b) results of a TEMPEST simulation of this arrangement showing power in the +1, −1, and zero diffraction orders as a function of mold–wafer offset. The mold is brought into alignment with the wafer by shifting it laterally until the +1 and −1 orders balance in intensity.

propagating plane wave at 365 nm wavelength after passing through the mold and reflecting from the wafer. The two-dimensional simulation domain used for the calculation is shown in Fig. 1(a). In the second step, the field incident on the photodetector was decomposed into its plane wave components, i.e., diffraction orders, with a Fourier transform. The results of the simulation, the power in the +1, −1, and zero diffraction orders as a function of offset (lateral displacement between mold and wafer) is shown in Fig. 1(b). This simple alignment-metrology technique works because the marked difference between the mold and wafer gratings (fused silica versus silicon) results in a strong blazing effect, i.e., the pumping of more power into the +1 diffraction order than into the −1 diffraction order. If, on the other hand, the mold and wafer gratings had been in similar materials, e.g., in fused silica and the surface oxide of silicon, the difference between the +1 and −1 diffraction orders would not change so rapidly with offset and such a simple alignment-metrology technique could not be used.

A sketch of a more robust alignment-metrology technique for imprint lithography, that works in almost all cases, is shown at the top of Fig. 2(a). In this case, the alignment marks consist of two equal-line-and-space gratings on the

mold and two more on the wafer for each of the two mutually orthogonal in-plane directions. The mold and wafer gratings are deliberately arranged to be out of phase with each other, the phase of the wafer grating on the left lags by 90° and on the right leads by 90°. The results of a ray-trace analysis of this alignment technique are shown at the bottom of Fig. 2(a). In this case, as the offset is increased, the power diffracted from the left-hand pair of gratings (dash–dotted curve) increases and the power diffracted from the right-hand pair of gratings (dashed curve) decreases. At perfect alignment, i.e., zero offset, the power diffracted by the two gratings pairs is equal. We recognize that a more accurate analysis of this alignment-metrology technique could have been obtained from a TEMPEST simulation, nevertheless, we believe that the results of our ray-trace analysis are qualitatively correct, at least to first order.

From an experimental point of view, determining correct alignment with a technique that relies on balancing two photodetector currents (one increasing and other decreasing) is superior to one that depends on locating an absolute minimum or maximum in current[6] because (i) the slope of the error signal (the difference divided by the sum) versus position is quite steep and (ii) the sign of the error signal gives the sign of the displacement directly. The largest source of error with this technique is the photodetectors. Care must be taken that the photosensitivity and the amplification factor of the two photodetectors are equal and vary identically with temperature. In practice, this is best done using a split photodetector in which the two detectors/amplifiers are on the same piece of silicon.

The other major source of error with this technique arises from wafer-grating asymmetry.[7] The alignment marks on the wafer tend to be degraded by overlying film layers and by other wafer processing steps such as etching and heat treatment. If the wafer gratings are asymmetrical, as shown at the top of Fig. 2(b), the alignment marks will not be aligned when the photocurrents are balanced. A plot of photodetector current (the sum of the +1 and −1 orders) versus offset, derived from a ray trace, is shown at the bottom of Fig. 2(b). The dotted lines in Fig. 2(b) show that the photodetector currents produced by diffraction from the two grating pairs illustrated at the top of Fig. 2(b) will not be equal at zero offset but will come into balance when the gratings are misaligned by approximately −20 nm. The dashed lines in Fig. 2(b) show that the photodetector currents produced by diffraction from two additional grating pairs, similar to those illustrated at the top of Fig. 2(b), but with the phase of the wafer grating on the left leading by 90° and on the right lagging by 90° [just the opposite of that shown at the top of Fig. 2(a)], will come into balance at an offset that is equal in magnitude but opposite in sign, i.e., at approximately +20 nm. In other words, the average offset of the two groups of blazed gratings, the solid lines in Fig. 2(b), will yield the same position as the single group of symmetric gratings, i.e., the correct alignment. Therefore, we claim that an accurate alignment-metrology technique for imprint lithography will require four grating pairs (mold and wafer) for each of the

Novel alignment system for imprint lithography

D. L. White and O. R. Wood II[a)]

Bell Laboratories, Lucent Technologies, 600 Mountain Avenue, Murray Hill, New Jersey 07974

A novel alignment system for imprint lithography in the deep sub-hundred nanometer realm is proposed. The new system is inherently more precise than the alignment systems used in conventional projection lithography because alignment marks on an imprint mold (the functional equivalent of a photomask in projection lithography) are directly compared to alignment marks on a wafer with no intermediate optics or reference points. If the measured misalignment is so severe that all marks cannot be brought into registration simultaneously by the usual $x-y$ translations and rotations, the mold is deliberately deformed with a system of piezoelectric actuators in such a way that its induced distortions precisely match those on the wafer and all of the alignment marks at each chip site can be pulled into registration simultaneously. Finite-element analysis indicates that using actuators to distort the mold is superior to distorting the wafer. © *2000 American Vacuum Society.* [S0734-211X(00)05406-8]

I. INTRODUCTION

Imprinting, one of the oldest pattern replication techniques, has been proposed as a possible future replacement for the projection lithography currently used in the production of semiconductor integrated circuits (ICs). The reasons for the renewed interest in this technology are its simplicity, its high-resolution capability, and its ready extendibility. In principle, the ultimate resolution is molecular in size—10 nm pillars have been produced and even finer detail on feature edges has been replicated.[1] The imprinting method most suited to IC applications involves the casting of a polymer against a rigid fused-silica mold that has a low-aspect-ratio pattern etched into its surface.[2] After the polymer is cured by exposure to ultraviolet radiation, the mold is removed and the pattern in the polymer layer is transferred into the surface of a silicon wafer via a thin organic planarizing/transfer layer by reactive ion etching.[3] This imprinting method has already been shown to possess sufficient resolution to take the technology down to 30 nm and below,[4] but before it can be used in this critical dimension range an alignment system that is accurate to considerably better than 10 nm must be devised. This is a daunting task, given that misalignment is already a leading cause of product failure in the IC industry.

Our strategy is to measure misalignment at a number of sites in the mold/wafer system and to attempt to bring all of them into registration simultaneously. If this is not possible because of distortions in the wafer or imperfections in the mold, the mold (or the wafer) is deliberately deformed in such a way that all alignment marks are within tolerance.

II. ALIGNMENT METROLOGY

In conventional projection lithography the mask is aligned to a reference mark on the mask stage and many different alignment marks on the wafer are aligned to a reference mark on the wafer stage. Some error is introduced when the relative position of these two secondary reference marks is determined during system calibration. Even though the positions of the stages' reference mirrors are measured to a small fraction of a wavelength with laser interferometers, the distances between those mirrors and the actual exposure sites on the mask and wafer may be tens of centimeters. Thus, any distortions, vibrations or thermal effects in the stages can also lead to image-placement errors. Mask and projection lens distortions are other possible sources of error.

In imprint lithography an alignment mark on the mold and the corresponding mark on the wafer are in close proximity, separated only by a few tens of nanometers. There are no intermediary projection optics. The alignment-system optics look directly at both marks simultaneously, so there are no inaccuracies introduced by secondary reference marks, $x-y$ stage errors, or projection lens distortions. A sketch of a possible alignment-metrology technique for imprint lithography, bearing some similarity to those developed previously for proximity x-ray lithography[5–7] and to *in situ* through-the-lens alignment systems,[8,9] is shown in Fig. 1(a). The alignment marks consist of one phase grating on the mold and another on the wafer for each of the two mutually orthogonal in-plane directions. The 600 nm period gratings have equal lines and spaces and are 50 nm deep. The mold and wafer are assumed to be separated by a 20 nm gap that is uniformly filled with a photopolymer having an index of refraction of 1.9. A laser or a collimated beam of light at 365 nm wavelength passing through the mold gratings is reflected from the wafer gratings and the total intensity of diffracted radiation is recorded with photodetectors (the zero-order beam is intercepted with a field stop). Alignment is determined by balancing the intensities of the $+1$ and -1 diffraction orders.
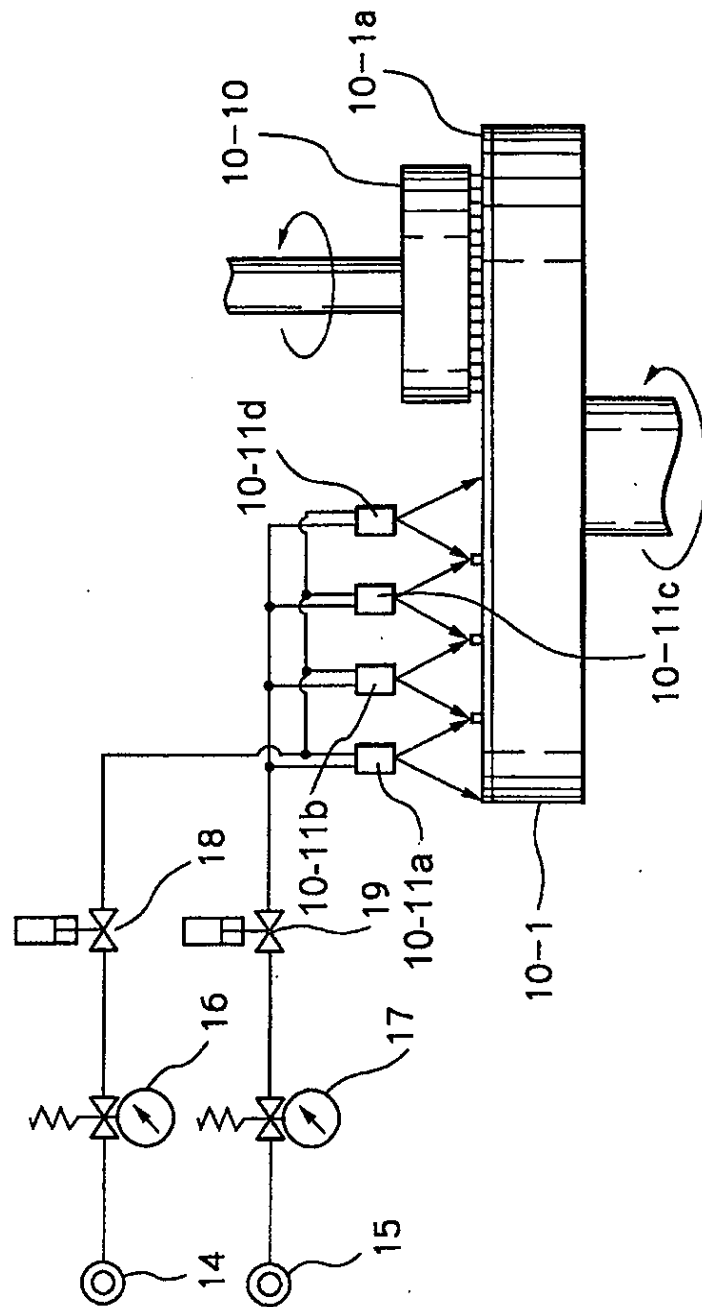
An accurate analysis of the system of phase gratings shown in Fig. 1(a) requires a rigorous finite-difference time-domain electromagnetic simulation since the two gratings are in each others' near field and, hence, function as a single optical diffractor. Such a simulation was carried out in two steps. In the first step, TEMPEST[10] was used to compute the electromagnetic field above the mold created by a downward

a)Electronic mail: orw@bell-labs.com

Fig. 4